Chapter 5

Energy, Exergy, Economic Performance Investigation of Heat Exchanger with Turbulators Inserts and THNF: An Experimental Study

Emergence in modified technologies requires rapid heat removal methods for better performance of the heat exchangers. For thermal improvement, passive inserts of twisted turbulator inserts (TTI), Perforated twisted turbulator inserts (PTTI) are used in the plain tube heat exchanger. This chapter focuses on the Energy, Exergy, and Economic sustainability effect of modified inserts with recent water-based ternary hybrid nanofluids (THNF).

5.1 Experimental procedure

Fig. 5.1. depicts the experimental setup's process layout schematic, which mostly consists of the radiator (dimensional details are presented in Table 5.1), a pump with a maximum capacity of 80lpm and a normal rated power of 746W at 2800RPM, control valves (to manage the flow rates), a reservoir tank, and a data indicator. Fig. 5.2. depicts the

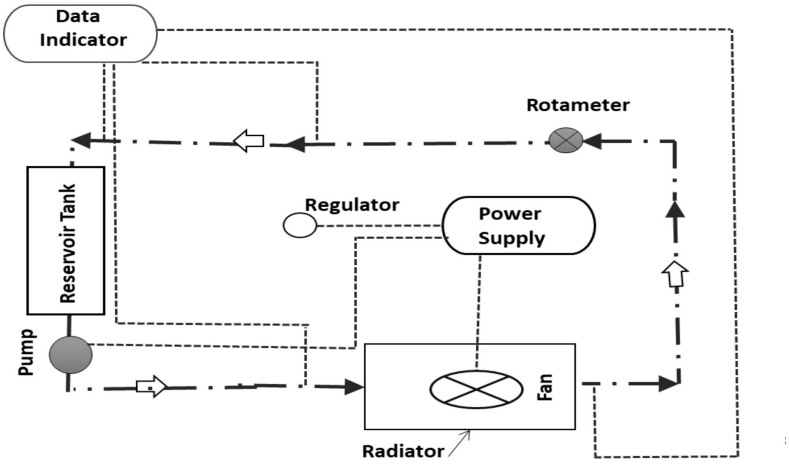

Fig. 5.1. Schematic of Experimental setup.

experimental setup, while Fig. 5.3. depicts a fin and tube radiator with precise dimensions.

Table. 5.1 Detailed dimensions of the radiator.

Description	Air side	THNF side
Pitch of fin	3.5mm	
Thickness of the fins	0.15mm	
Diameter of tube (d_{tube})		9mm
Thickness of tube		0.5mm
Longitudinal Pitch Transverse Pitch	19.6mm 24.8mm	
Frontal length of radiator, $L_{radiator}$	340mm	
Frontal width of radiator,$W_{radiator}$	320mm	
Frontal width of the fin, W_{fin}	54.2mm	
Net heat transfer surface area/net volume	$80.35m^2m^{-3}$	$3.31m^2m^{-3}$

Total tubes (N_{tube}) are 36, and Total fin (N_{fin}) are 96.

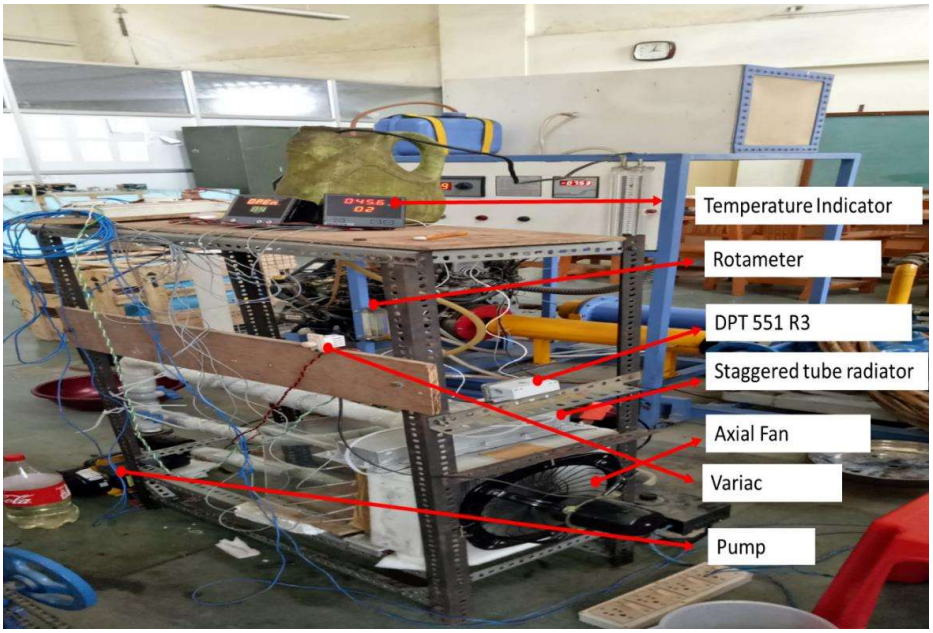

Fig. 5.2. Details of the experimental setup.

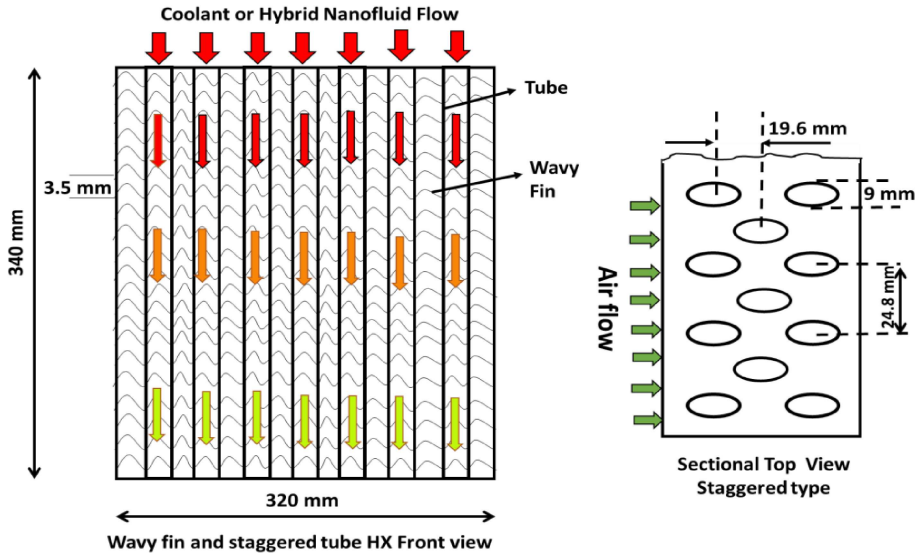

Fig. 5.3. Front and top view of fin and tube radiator.

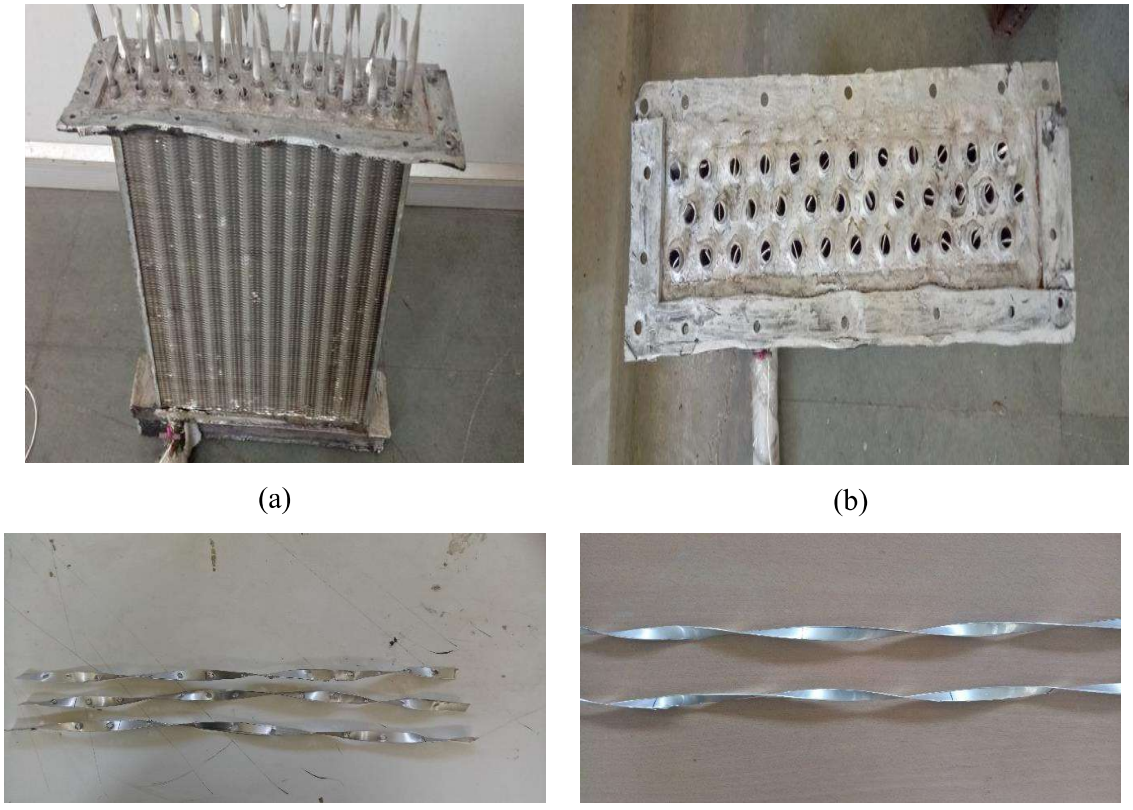

(a) (b)

(c) (d)

Fig. 5.4. Modified inserts to the radiator, (a) tube inserts in heat exchanger; (b) top view of inserts in heat exchanger; (c) Perforated tube inserts; (d) Twisted tape inserts.

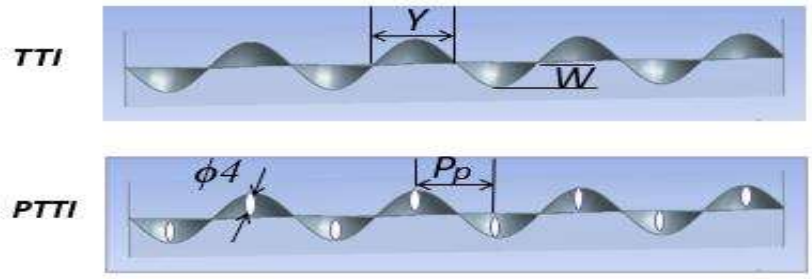

Fig. 5.5. Dimensional and pictorial configuration of modified turbulators inserts [TTI, PTTI].

Table. 5.2 Detail dimensions of Turbulator inserts.

Turbulators	**Y**	**W**	**Y/W**	**P_p**	**P_p/Y**	**Inserts t_i Thickness**
TTI	85mm	5mm	17	____	___	0.5 mm
PTTI	85mm	5mm	17	20mm	0.25	0.5 mm

The experimental study is conducted for four different fluid compositions (water, 0.06%, 0.09%, and 0.12% THNF) at volume flow rates (10lpm - 26lpm) for corresponding Reynolds number (3200-7500) on fixed air frontal velocity (5m/s) recorded with precalibrated hot wire testo probe anemometer. Also, modified turbulator inserts of TTI and PTTI inserted in the tube side for heat transfer enhancement as shown in Fig. 5.4. Pictorial representation of the turbulator inserts is also shown in Fig. 5.5. Detailed dimensions of the modified turbulator inserts of TTI and PTTI is listed in Table 5.2. For the experimental investigation, prepared 4 liters of the volume of hybrid nanofluid is kept in the reservoir tank. The centrifugal pump is used to supply the hybrid nanofluid to the radiator at different volume flow rates operated using control valves. A thermostat is kept on to maintain the fluid temperature at 70°C. The hot fluid enters the radiator and exchanges heat from the air and gets cooled at the radiator outlet. The data is recorded while the radiator parameter changed. Five thermocouples are positioned at the air side radiator outflow to measure the average air temperature per ASHRAE guidelines. Two thermocouples are fitted to measure the temperature

of the hot fluid entering and leaving the radiator. Exit air temperature is measured, and mean air temperature is used for analysis. A quartz thermometer is used to calibrate every thermocouple.

5.2 Data Reduction

The equations used to obtain the radiator's geometrical parameter is given as (5.1-5.10).

The tube's peripheral area ($A_{Peripheral}$) is determined by,

$$A_{peripheral} = N_{tube} \Pi d_{tube} L_{radiator} \tag{5.1}$$

The area of the tube (A_{tube}) is determined by,

$$A_{tube} = \frac{\Pi}{4} d_{tube}^2 \tag{5.2}$$

The peripheral area (P_{tube}) is calculated by,

$$P_{tube} = \Pi d_{tube} L_{raadiator} \tag{5.3}$$

Radiator frontal area ($A_{radiator}$) is determined by,

$$A_{radiator} = W_{radiator} L_{raadiator} \tag{5.4}$$

Peripheral area of a fin (A_{fin}) is given by,

$$A_{fin} = 2 W_{radiator} W_{fin} \tag{5.5}$$

The tube base surface area (A_{base}) is given by,

$$A_{base} = d_{tube} \Pi (L_{radator} - 2 H_{fin} N_{fin}) \tag{5.6}$$

Single tube fin and base surface area ($A_{fin,base}$)is determined as,

$$A_{fin,base} = A_{fin} N_{fin} + A_{base} \tag{5.7}$$

Hydraulic diameter (D_h), total internal ($A_{internal}$), external ($A_{external}$) surface area is determined by

$$D_h = \frac{4 A_{tube}}{P_{tube}} \tag{5.8}$$

$$A_{internal} = A_{peripheral} N_{tube} \tag{5.9}$$

$$A_{external} = A_{fin,base} N_{tube} \tag{5.10}$$

5.3 Performance parameters evaluation

The heat transfer of hot fluid in tube side (Q_f) is determined by

$$Q_f = \dot{m}_f c_{p,f} (T_{fi} - T_{fo}) \tag{5.11}$$

Where $\dot{m}_f = \rho_f * VFR$, and VFR is the volume flow rate.

The heat transfer coefficient (h_f) of hot fluid is determined by

$$h_f = \frac{Q_f}{A_{peripheral} * N_{tube} * (T_b - T_w)} \quad (5.12)$$

T_b is computed as the average of the entrance and exit coolant temperatures and Tw is the wall temperature is evaluated (**Goudarzi et al. 2017**) as

$$T_w = 0.33 * (T_{fi} + T_{fo} + T_{ai}) \quad (5.13)$$

The airside heat transfer mechanism is provided by

$$Q_a = \dot{m}_a c_{p,a} (T_{ae} - T_{ai}) \quad (5.14)$$

Where $\dot{m}_a = \rho_a A_{radiator} V_a$, represents air mass flow, V_a is the frontal air velocity and ρ_a is air density (1.2kgm^{-3}).

The calculation of the total heat exchange across the radiator (Q_t) as,

$$Q_t = \frac{Q_f + Q_a}{2} \quad (5.15)$$

Reynolds number (Re_f) of hot fluid is determined as,

$$Re_f = \frac{\rho_f V_{max} D_h}{\mu_f} \quad (5.16)$$

Once the pressure drop has been measured, the minor pressure drop (Δp_{minor}) is reduced and then the friction factor (*ff*) is determined by,

$$\Delta p = \Delta p_{exp} - \Delta p_{minor} \quad (5.17)$$

$$\frac{\Delta p_{minor}}{\rho_f g} = \frac{v_1^2}{2g}\left(1 - \left(\frac{A_1}{A_2}\right)\right)^2 + kf_1 \frac{v_3^2}{2g} + \frac{v_3^2}{2g}\left(1 - \left(\frac{N_{tube} A_3}{A_4}\right)\right)^2 + kf_2 \frac{v_5^2}{2g}$$

Where, $A_1 = A_5$, $A_2 = A_4$ and $v_1 = VFR / A_1$, $v_3 = VFR / (N_{tube} A_3)$, $A_3 = \frac{\Pi}{4} * D_h^2$,

$kf_1 = A_3 / A_2$, $kf_2 = A_5 / A_4$, A_1, A_2, A_3, A_4, A_5, is corresponding sectional area and

velocity with kf_1 and kf_2 is area ratio. Also, V_1, V_2, V_3, V_4 and V_5 represents corresponding sectional velocities as shown in Fig. 5.6.

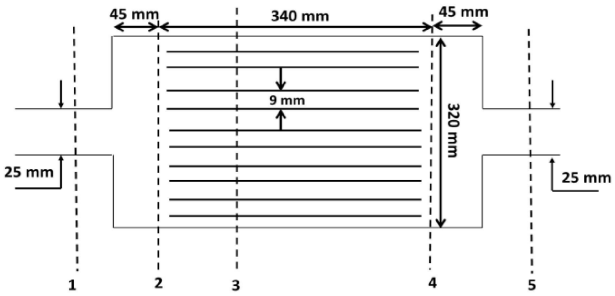

Fig. 5.6. Sectional view of the heat exchanger.

$$ff = 2\frac{\mathrm{D_h}}{\mathrm{L_{radiator}}\,\rho_f \mathrm{V_f}^2}\frac{\Delta \mathrm{P}}{} \tag{5.18}$$

And, the non-dimensional Nusselt number of hot fluid is calculated to be

$$Nu = \frac{\mathrm{h}_f \mathrm{D}_h}{\mathrm{k}_f} \tag{5.19}$$

Now, UA, also known as the total HX coefficient, is represented as,

$$\frac{1}{UA} = \frac{1}{\eta_o h_a A_a} + \frac{1}{h_f A_f} + \frac{\ln(\frac{d_0}{d_i})}{2\pi L k_t} \tag{5.20}$$

Whereas the effectiveness of HX surfaces is assessed as,

$$\eta_o = 1 - \frac{A_{fin}}{A_a}\left(1 - \eta_{fin}\right) \tag{5.21}$$

Fin efficiency of wavy structured is evaluated as,

$$\eta_{fin} = \frac{\tanh\left(\sqrt{2 * \frac{h_a}{k_{fin} t_{fin}}}\, r\theta\right)}{\sqrt{2 * \frac{h_a}{k_{fin} t_{fin}}}\, r\theta} \tag{5.22}$$

Where different non- dimensional parameters are determined as,

$$\theta = \left(\frac{R_{eq}}{r} - 1\right) * \left(1 + 0.35\left(ln\frac{R_{eq}}{r}\right)\right) \tag{5.23}$$

$$\frac{R_{eq}}{r} = 1.27 * \left(\frac{S_l}{S_m} - 0.3\right)^{0.5} \tag{5.24}$$

$$S_m = P_l/2 \quad \text{and} \quad S_l = \sqrt{\left(\frac{P_t}{2}\right)^2 + \left(\frac{P_l}{2}\right)^2} \tag{5.25}$$

Pumping power in the tube side, with fan and tube pumping efficiency, assumed to be 65%, is used to calculate the energy consumption needed to operate an HX efficiently.

$$P_{pp} = \frac{\Delta p_f \times VFR}{\eta_p} \tag{5.26}$$

$$F_{PP} = \frac{A_{radiator} \times V_a \times \Delta p_a}{\eta_p} \tag{5.27}$$

After the thermal and hydraulic performance, a non-dimensional parameter, performance index (PI) is evaluated as,

$$PI = \frac{Q_t}{P_{PP} + F_{PP}} \tag{5.28}$$

Entropy analysis suggests the details about the degradation of qualitative energy, entropy generation mainly occurs due to thermal change, and viscous change due to pressure drop. The total entropy generation for the present investigation is calculated by,

$$S_{gen} = \dot{m}_a \left[c_{p,a} \ln \frac{T_{a,e}}{T_{a,i}} - R_a \ln \frac{p_{a,e}}{p_{a,i}} \right] + \dot{m}_f \left[c_{p,f} \ln \frac{T_{f,e}}{T_{f,i}} - \frac{\Delta p_f}{\rho_f T_{f,mean}} \right] \tag{5.29}$$

Availability of energy is analyzed through exergy, air takes energy from the hotter fluid passing through the tube. So exergy gain by air is evaluated as,

$$\Delta Ex_a = Q - T_0 \left[\dot{m}_a c_{pa} \ln\left(T_{a,e}/T_{a,in}\right) + \dot{m}_a R \ln\left(p_{a,in}/p_{a,e}\right) \right] \tag{5.30}$$

Hot fluid in the tube side losses energy, and exergy loss by the hot fluid in the tube side is evaluated as,

$$\Delta Ex_f = Q + T_0\left[\dot{m}_f c_{p,hnf} \ln\left(T_{f,in}/T_{f,e}\right) - \dot{m}_f \Delta p_f/(\rho_{hnf} T_{f,mean})\right] \tag{5.31}$$

After the exergy analysis, exergy efficiency, also known as second law efficiency is determined as,

$$\eta_2 = \frac{\Delta Ex_a}{\Delta Ex_f} \tag{5.32}$$

Irreversibility is determined as,

$$I = T_0 S_{gen} \tag{5.33}$$

The exergy ratio-based sustainability index (SI), which has been studied to determine the ultimate application of resources, Sustainability index indicates the effective energy utilization. Higher the sustainability index better the utilization of energy occurs is given as,

$$SI = \frac{1}{(1-\eta_2)} \tag{5.34}$$

Nusselt ratio has been established as the heat transfer enhancement coefficient based on the various turbulators employed in the experiment. It indicates the increase in heat as a result of altered geometry. In comparison to the Nusselt number with a plain tube, heat transfer enhancement for various turbulators is defined as,

$$Nu_r = \frac{\left(Nu_f\right)_{TTI/PTTI}}{\left(Nu_f\right)_{PT}} \tag{5.35}$$

Due to the usage of various turbulators, the pressure drop penalty is increased at the expense of heat enhancement. The relative pressure drop penalty coefficients for various inserts are defined as,

$$f_r = \frac{\left(f_f\right)_{TTI/PTTI}}{\left(f_f\right)_{PT}} \tag{5.36}$$

To measure heat transfer improvement for a specific pumping power consumption, the performance evaluation criterion (PEC) includes the heat transfer enhancement coefficient and relative pressure drop coefficient ratios. PEC was studied at an equal power consumption level to assess the practical luxury of turbulator inserts in air HX. For plain tubes HX and turbulator inserts HX, the mathematical expression of PEC requirement is determined as,

$$PEC = \frac{Nu_r}{\left(f_r\right)^{\left(\frac{1}{3}\right)}} \tag{5.37}$$

Heat exchangers' performance is improved by using different inserts and THNFs at the expense of pumping power. One of the main criteria for analysis will be power consumption in terms of CO_2 discharge. The primary power substation receives its electricity from coal-based power generation. Carbon emission factors may be used in CO_2 discharge analysis. CO_2 discharge (**Caliksan et al. 2012**) is determined as,

$$Dis_{CO_2} = \frac{f_{CO_2} P_{Net} t_{run}}{10^6} \tag{5.38}$$

Where Dis_{CO_2} is the carbon discharge factor, which is represented by the amount of carbon dioxide released annually, P_{net} which is the net power consumption in kW required to run the equipment for an hour, and t_{run} is the heat exchanger's yearly working time (h/Annum), f_{CO_2} are taken to be 0.820 $kgCO_2/kWh$ (location-based) for the carbon discharge factor. Net electricity usage determines heat exchanger operating cost (HX_{OC}) , which are calculated as,

$$HX_{OC} = P_{Net} t_{run} C_{electricity} \tag{5.39}$$

Heat exchangers have been assumed to operate continuously for 180 days out of the year before maintenance, or twenty-four working hours each day. The price of electricity has been calculated at 8 per kWh.

5.4 Experimental procedure and validation

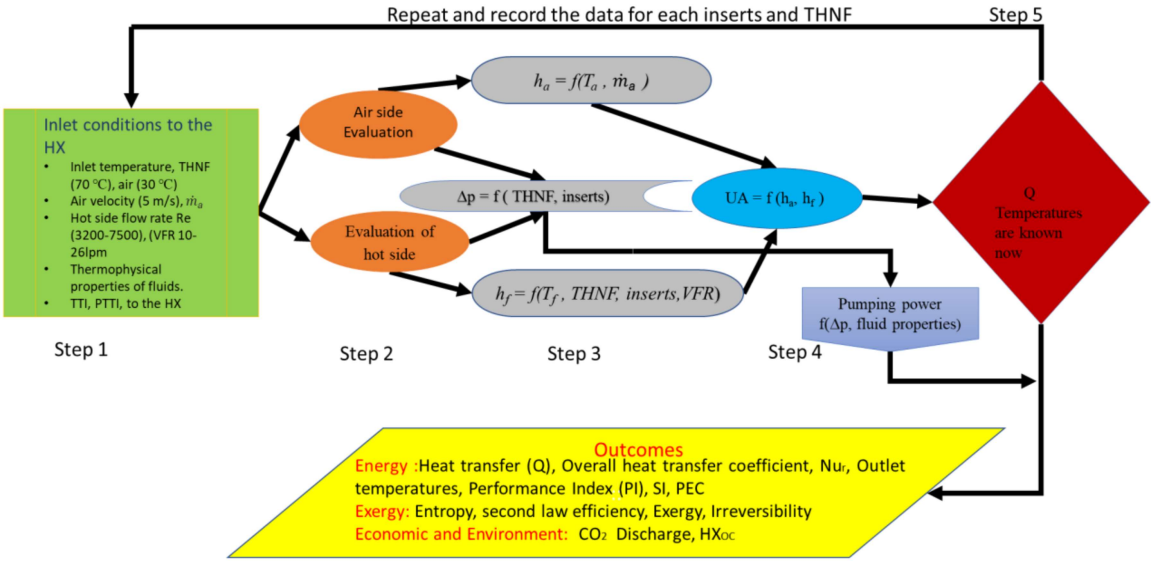

Fig. 5.7. Flow chart outline of experimental procedure outcome.

Following is a description of the step-by-step experimental chronology of the current investigation's results:

Step 1: The initial intake condition for air HX has been assigned as fluids entry temperatures (T_{fi} = 70°C, T_{ai} = 30°C), VFR (10 - 26lpm) with corresponding Reynolds number (3200-7500), and THNF with constant air velocity 5m/s.

Step 2-5: Using the sufficient experimental recorded data (pressure drop, temperatures), convection heat transfer coefficient for air and THNF's, overall heat transfer coefficient, heat transfer, and friction factor is evaluated.

Step 6: Experimentation is carried out to ascertain the heat transfer coefficient, air side, hot fluid side, and pressure drop for the different tube inserts and fluids. Later, the performance outcomes based on energy, exergy, carbon discharge, and operating cost are evaluated for the combination. The step-by-step chart outline of the experimental procedure is shown in Fig. 5.7.

5.4.1 Verification and validation

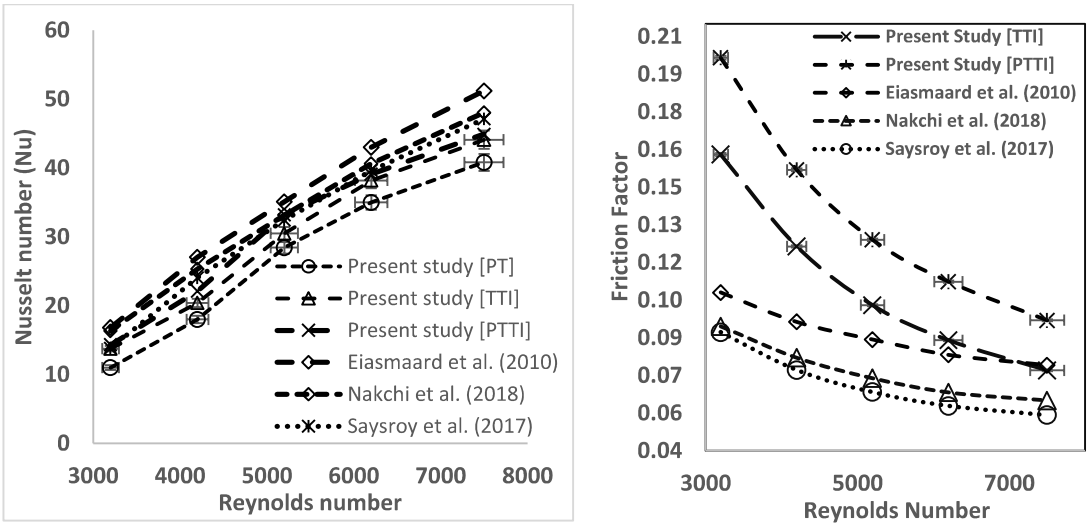

(a) (b)

Fig. 5.8. Experimental validation, (a) Nusselt number with Reynolds number; (b) Friction factor with Reynolds number for water.

The present study of different inserts for Nusselt number and friction factor has been compared to the available results as presented in the Fig. 5.8. Nusselt number for different inserts and plain tube shows a likewise trend of variation with Reynolds number as shown in Fig. 5.8. (a). At lower Reynolds number the deviation is high and at a higher Reynolds number 7500, the Present study of TTI, and PTTI show 6.8% and 6.9% deviation compared to **Saysroy et al., 2017**, and **Nakchi et al., 2018,** respectively. Also, the trend of Nu variation obtained is similar to the **Eiasmaard et al., 2010**. However, when compared to available study, the present study of the friction factor shows similar trend of decrement with increased Reynolds number as shown in Fig. 5.8. (b). At a lower Reynolds number, the fluctuation of the present study is high but at a higher

Reynolds number of 7500, on the comparison, the Present study of PTTI shows a 19% higher friction factor compared to **Eiasmaard et al., 2010**. Based on the trend of the Nusselt number and friction factor of the present study shows similar variation with the available results.

5.5 Uncertainty investigation

Analysis of the uncertainty for several parameters, including the heat transfer coefficient, the heat transfer dependent on temperature, flow rate, and other independent parameters. The experiment uncertainty for several variables has been assessed (**Moffat 1988, Krishnamoorthi et al., 2018, Ağbulut et al., 2020, Singh et al., 2020.**). The dependent parameter U in the equation is a function of the independent variables $y_1, y_2, \ldots\ldots\ldots, y_n$ and their relative uncertainties are denoted by the letters u_1, u_2, and u_n. The uncertainty, denoted by the symbol U_R, is determined as follows:

$$U_R = \left[\left(\frac{\partial R}{\partial y_1} u_1 \right)^2 + \left(\frac{\partial R}{\partial y_2} u_2 \right)^2 + \ldots\ldots\ldots\ldots\ldots + \left(\frac{\partial R}{\partial y_n} u_n \right)^2 \right]^{1/2} \tag{5.28}$$

The calculation for the heat transfer's uncertainty is

$$\delta Q = \sqrt{\left(\frac{\partial Q}{\partial m} \delta m \right)^2 + \left(\frac{\partial Q}{\partial C_p} \delta C_p \right)^2 + \left(\frac{\partial Q}{\partial T_{in}} \delta T_{in} \right)^2 + \left(\frac{\partial Q}{\partial T_{out}} \delta T_{out} \right)^2} \tag{5.29}$$

Table. 5.3 Instrument accuracy and uncertainty in derived experimental quantities.

Instruments/ parameter	unit	Uncertainty/accuracy
Coolant flow rate	L min^{-1}	±1
Temperature	°C	±0.1
Testo probe anemometer	ms^{-1}	±0.1
Heat transfer coefficient	$Wm^{-2}K^{-1}$	±3-5%
Coolant Reynolds Number	-	±3.2%
Heat transfer	W	±3.5%
Δp	Nm^{-2}	±0.2%
Velocity	m/s	±0.78%
Thermal conductivity	W/mK	±2.0%
Viscosity	Pa.s	±2.0%
Density	Kg/m^3	±2.0%
Specific heat capacity	J/kgK	±2.0%

5.6 Results and discussion

5.6.1 Effect of flow and inserts on the Thermal performance

Figure 5.9. and 5.10. displays the effects of turbulator inserts on heat transfer and Nusselt ratio with Reynolds number of ternary hybrid nanofluid at the different concentrations used in wavy finned tube HX. The Heat transfer and Nusselt ratio typically follow a linear relationship with the Reynolds number. Increased turbulence intensity, which also contributes to an increased convective heat transfer coefficient, is the main cause of linear variation of heat transfer. When inserts are employed in air HX, turbulators greatly increase the Nusselt number but the Nusselt ratio decreases with the increase in flow, as a lower Reynolds number the thermal change is more dominant than viscous and vice versa phenomenon occurs at a higher Reynolds number. However,

turbulators produced a radial intensive fluid mixing that is not often seen in PT HX. The creation of swirl flow, thermal boundary layer interruption, and radial pressure gradient is the main causes of the increase in heat transfer and Nusselt ratio in the presence of turbulators in HX. Mainly among the turbulators, PTTI promotes the strength of fluid intermixing at the perforations and with thin and redevelopment in the thermal boundary layer obtains the highest heat transfer. The presence of perforated holes permits an interruption in the fluid flow direction, which induces regeneration of the boundary layer close to the perforated holes and enhances the heat transfer and Nusselt ratio. However, among turbulators, PTTI in HX shows a bigger improvement than TTI. Among the working fluid, the higher concentration of hybrid nanofluid of 0.0012, shows significant enhancement in heat transfer and is quite lower for a lower concentration of hybrid nanofluid due to their better thermal conductivity. At the lowest Reynolds number, 3200, PTTI and TTI with 0.12% volume concentration of THNF show 36.5% and 25.8% higher heat transfer than without inserts with water. Also, PTTI and TTI with 0.12% volume concentration of THNF show 1.38 and 1.26 times higher Nusselt number than a plain tube with water, respectively.

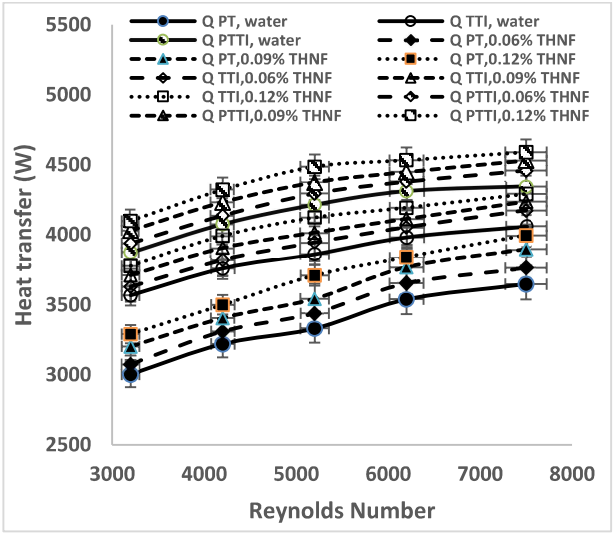

Fig. 5.9. Heat transfer with Reynolds number for different inserts and working fluids.

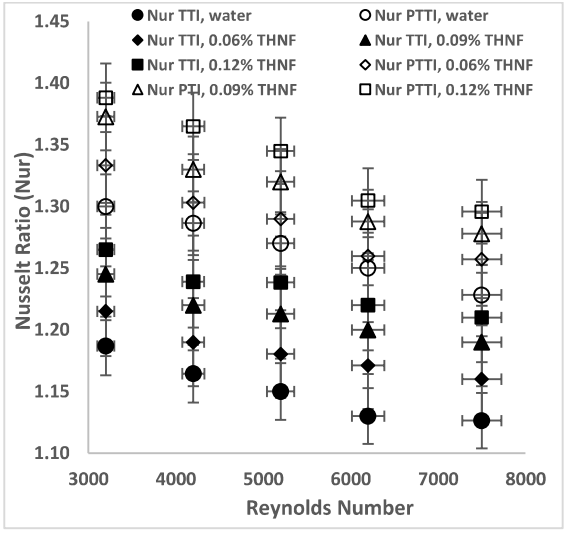

Fig. 5.10. Nusselt ratio with Reynolds number for different inserts and working fluids.

The benefits and practical applications of the air HX with various turbulator inserts are identified by performance evaluation criteria or thermal performance factors. PEC represents the energy utilization in a heat exchanger for fixed power input. PEC variation for different inserts and coolants is presented in the Fig 5.11. PEC greater than unity is regarded as an energy-saving measure in terms of performance improvement and obtained greater than unity for all the cases examined. PTTI in HX shows the highest PEC of 1.075 for the different investigated hybrid nanofluids. PEC shows decrement with the increased flow rate. This is mainly because when there are turbulators present, thermal enhancement predominates over friction factor at a lower Reynolds number. In addition, an examination of the various hybrid working fluids used in HX with different inserts revealed a small but considerable variance in PEC. Turbulators also served to improve the heat transfer between hot fluids (THNFs) and air in an HX. With the help of various inserts, hotter fluid can transmit heat to the air more quickly. As of right now, Turbulator inserts significantly improve heat transmission while using Lower Reynolds numbers. Tube side working fluid also termed as hot fluid, lowers the temperature drop due to energy exchange between the hot fluid and cold fluid (air). At a lower Reynolds number, due to higher residence time for energy exchange among the fluid, the temperature drop is larger. And with the increased Reynolds number the temperature drop reduces due to not having enough time for the energy exchange. Figure 5.12. shows the hot fluid outlet temperature with Reynolds number for different inserts and fluids. Residence time decreased as the flow rate increased, reducing the temperature drop. However, with turbulator inserts, the radial fluid flow direction is enhanced, allowing the hot fluid in the tube core to impact the tube wall surface and heat the air. Also, PTTI promotes the intermixing of the fluid from the core to the wall surface and enables a larger temperature drop. PTTI with 0.12% THNF, shows a 1.9°C further lower drop compared to without inserts with water as a working medium.

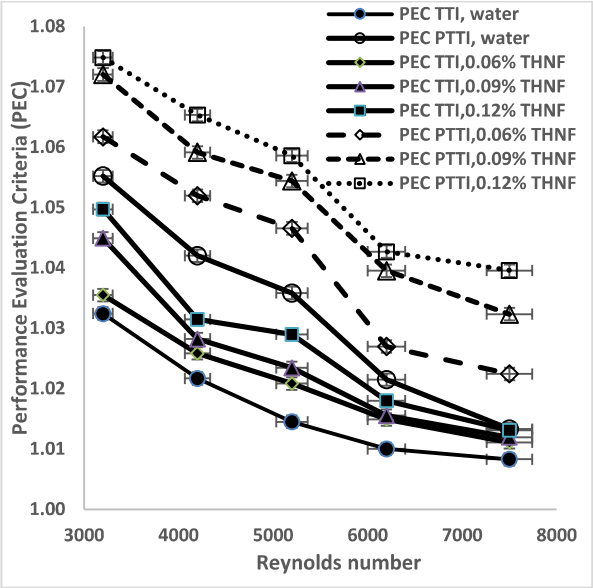

Fig. 5.11. PEC with Reynolds number for different inserts and working fluid.

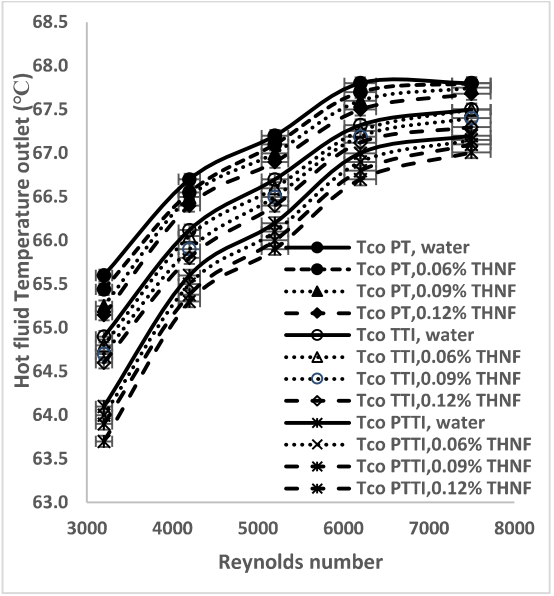

Fig. 5.12. Coolant outlet temperature with Reynolds number for different inserts and working fluid.

The Performance index is another parameter that takes into account of the combined impact of heat transmission and the amount of power needed to run a HX. Fig. 5.13. at Re 3600 shows the performance index of air HX with various geometrical alterations and hybrid nanofluids. Due to the presence of perforation on twisted turbulators, PTTI delivers higher swirl generation and boundary layer disruption, which improves heat transfer further than TTI and plain tube air HX. Therefore, when PTTI in air HX is investigated, the Performance index is obtained to be the highest. For comparison, at 3200 Reynolds number, PTTI shows 39.8%, and TTI shows 21.3% higher performance index using 0.12% THNF as working fluid compared to without inserts water as working fluid. Figure 5.14. compares the effects of various turbulators inserts with Reynolds number to a plain tube configuration of the overall heat transfer coefficient of the HX with 0.12% THNF as a working fluid. Turbulators generate swirl flows and exert a centrifugal force on the tube wall. Additionally, fluid residence time and enhanced mixed fluid flow between the tube surface and core area amplify the secondary flow, making the overall heat transfer coefficient of

turbulators greater for each Reynolds number than that of a plain tube. The fact that TTI interrupts the boundary layer near the twisted tape and increases the fluid flow's residing time, while perforated twisted turbulators also cause interruptions in the boundary layer near their perforations and more radial fluid flow could be the cause of increased overall heat transfer coefficient. Among tube inserts, at 3200 Reynolds number, PTTI shows 23.3% and TTI shows 17.3% higher overall heat transfer coefficient with 0.12% THNF compared to without inserts with water as working fluid.

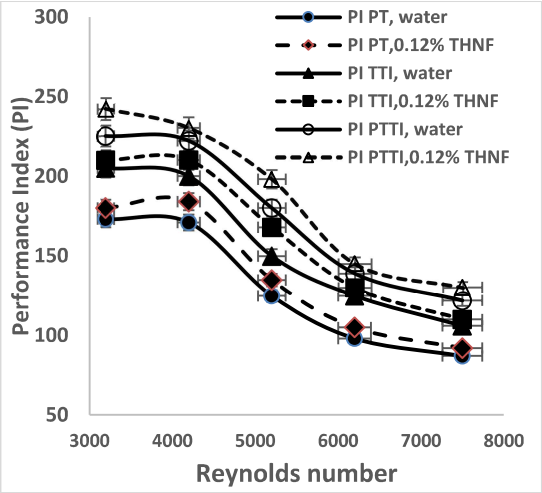

Fig. 5.13. Performance Index with Reynolds number for different inserts and working fluids.

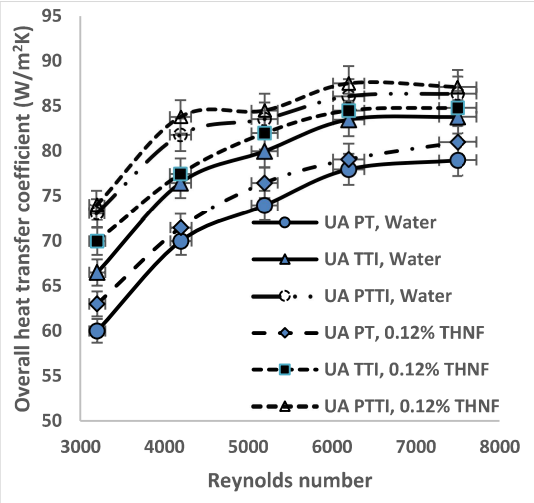

Fig. 5.14. Overall heat transfer heat transfer coefficient with Reynolds number for different and working fluids.

5.6.2 Effect of flow and inserts on pressure drop

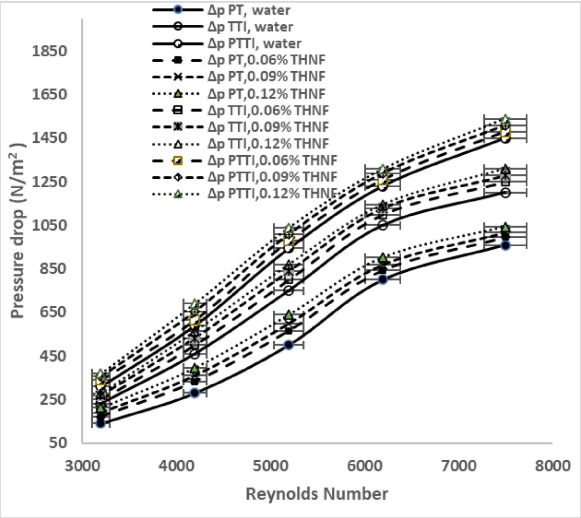

Fig. 5.15. Pressure drop with Reynolds number for different inserts and working fluids.

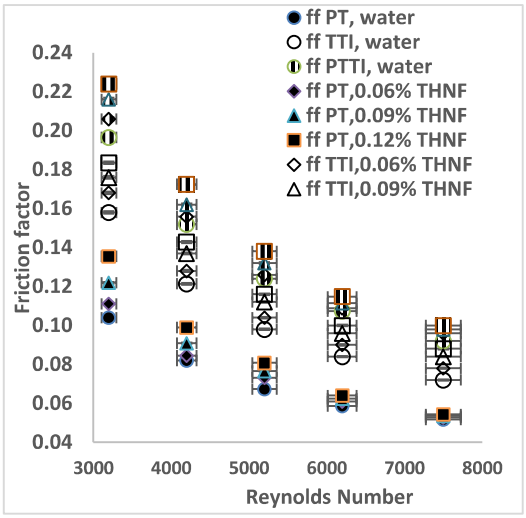

Fig. 5.16. Friction factor with Reynolds number for different inserts and working fluids.

Significant augmentation happens with a penalty in pressure. Figure 5.15. illustrates the pressure drop fluctuation with the Reynolds number for various inserts for THNF. Similar to the plain tube with Reynolds number, the pressure drop fluctuation trend for turbulators is also observed to be the same. As Reynolds number rises, pressure drop also rises. Greater pressure drop is shown by the turbulators insert than by the plain tube. Turbulators produce a significant amount of secondary flow, which when combined with high fluid obstruction and viscosity loss inside tubes with inserts results in a greater pressure drop. Additionally, at lower Re, the pressure drop is smaller, whereas, at higher Re, the pressure drop is enormous due to greater interaction between the inertial force and pressure force at the boundary layer. However, Fig. 5.16 shows the friction loss due to the presence of with and without turbulators with Reynolds numbers between (3200-7500). The plain tube and turbulators insert both exhibit equal reductions in frictional loss according to curve trends. However, as the Reynolds number rises, the friction factor gradually decreases. At lower Re, strong frictional forces are present at the rear of twisted turbulators,

enhancing the production of vortices and leading to greater friction loss. Turbulators have a larger friction factor than plain tube. The main causes of frictional drag include an increased surface area when turbulators are present, amplified swirl intensity, and the loss of greater viscosity areas near the tube surface. For comparison with 0.12% THNF as working fluid, PTTI requires 80% to 98% higher frictional factor, TTI requires 50% to 76% higher frictional factor compared to plain tube HX with water as working fluid at highest and lowest Reynolds number, respectively.

5.6.3 Effect of flow and inserts on exergy

The minimal entropy and mean entropy principles inside HX are necessary for a detailed second law analysis. Figure 5.17. illustrates the use of qualitative energy for THNF at various Reynolds numbers under various geometrical alterations in terms of exergy change of coolant of the HX. The exergy change in the coolant shows a significant improvement with turbulators inserts at a lower Reynolds number. This is because inserts in the plain tube restrict flow and cause blockage, which increases residence time and results in a higher exergy exchange between the fluids than air HX of the plain tube. Additionally, because PTTI results in stronger exergy exchange due to the radial direction with intermixing of fluid flow dominance over TTI in turbulators, exergy exchange is intensified further. Higher Reynolds number, however, an improvement in exergy exchange persisted because of an increase in turbulence intensification, even though the rate of increment remained lower due to viscous entropy generation's dominance over thermal entropy. The hot fluid is cooled and hence termed a coolant, Exergy change is also a crucial parameter that needs to investigate.

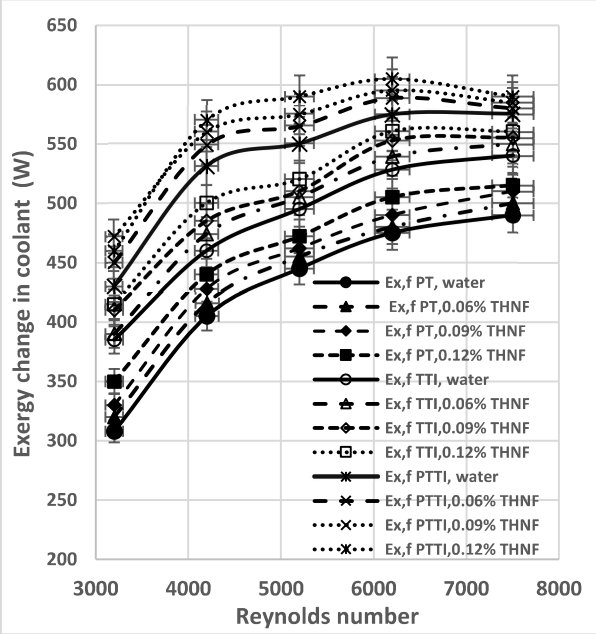

Fig. 5.17. Exergy change with Reynolds number for different inserts and working fluids.

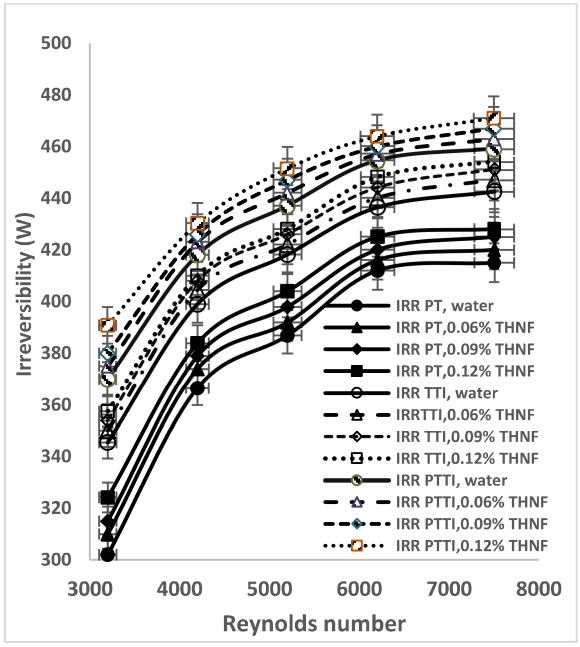

Fig. 5.18. Irreversibility with Reynolds number for different inserts and working fluids.

With 0.12% THNF as working fluid and at 3200 Reynolds number, PTTI shows 49.4% and TTI shows 34.4% higher exergy change compared to the plain tube with water as working fluid. Irreversibility also refers to the variance in energy loss between heat-exchanging fluids. It is observed that even turbulators insertion causes more irreversibility than without inserts. Since irreversibility is related to entropy generation, which is proportional to the mass flow rate, the trend with respect to irreversibility increases with Re as shown in fig 5.18. As PTTI exhibited highest and lowest for plain tube while an intermediate variation in TTI air HX of examined working fluids, a typical order of increased heat transfer and pressure drop followed. This is because PTTI produces enough extra vorticity to regenerate the boundary layer at the perforated positions while missing in the case of TTI. Irreversibility also refers to the variance in energy loss across heat-exchanging fluids. It is obtained that even turbulators insertion causes more irreversibility than they would without them. For comparison, at the lowest Reynolds number 3200 using 0.12% THNF shows 28.4% and 18.9% higher irreversibility for PTTI and TTI, compared to without inserts with water as working fluid respectively.

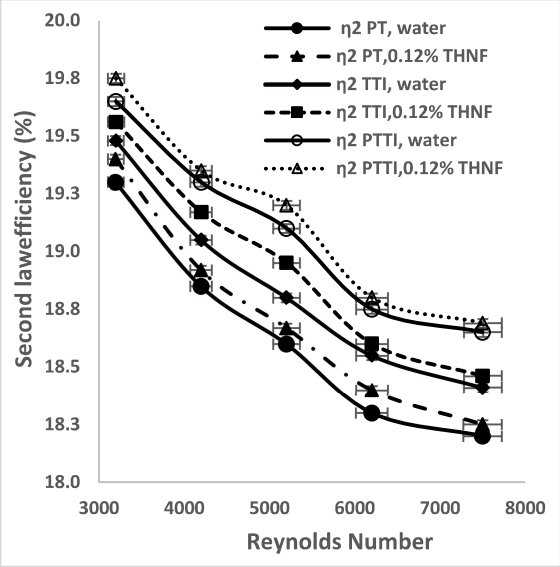

Fig. 5.19. Second law efficiency with Reynolds number for different inserts and working fluids.

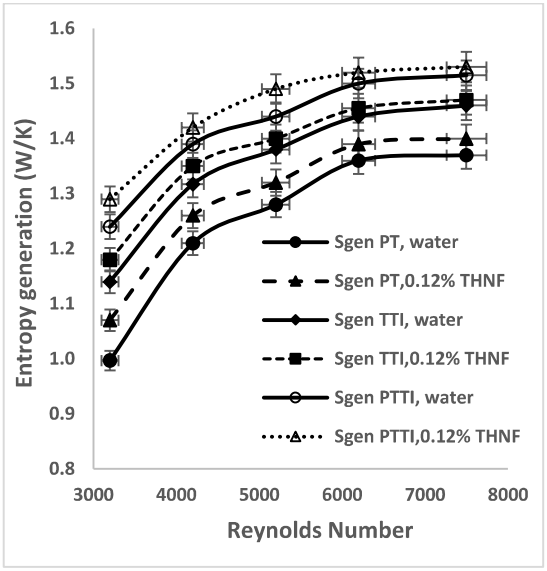

Fig. 5.20. Entropy generation with Reynolds number for different inserts and working fluids.

Exergetic efficiency, often known as second law efficiency, refers to the use of quality energy to improve thermal system components. Higher efficiency interprets to a better HX thermal design. However, various turbulators significantly increased exergetic efficiency compared to HX with simple tubes, and this is because the hot fluid (THNF) lost more energy than it gained from the air as shown in fig. 5.19. However, of inserts, PTTI in HX, working fluid investigated, displaying the highest second law efficiency compared to other inserts, while the lowest obtained for PT HX, as energy utilization and exergy exchange betters in PTTI than TTI, therefore energy utilization raises better. Thus, a HX with various turbulators inserts effectively aimed at a better thermal device. For the cases investigated, second law efficiency trend shows decrement with the increment in Reynolds number. However, at 3200 Reynolds number, PTTI shows 2.3% and TTI shows 1.8% higher second law efficiency using 0.12% THNF than plain tube with water as working fluid. Additionally, Fig. 5.20 illustrates another parameter as entropy generation variation with Reynolds number for different turbulator inserts. Entropy generation is dependent upon thermal entropy and viscous entropy. Although higher Reynolds number viscous entropy

generation predominates over thermal entropy generation. With the increment in Reynolds number, both the viscous and thermal entropy generation of the fluids increases. Therefore, when the Reynolds number increases, more entropy is generated. For comparison at 4200 Reynolds number, 17.8% and 12.7% higher entropy are generated for PTTI and TTI, respectively, with 0.12% THNF than a plain tube with water as working fluid. The results imply that a superior design of compact HX is accomplished with turbulators since the entropy generation increase was relatively still less than the heat transfer enhancement of HX with varied inserts.

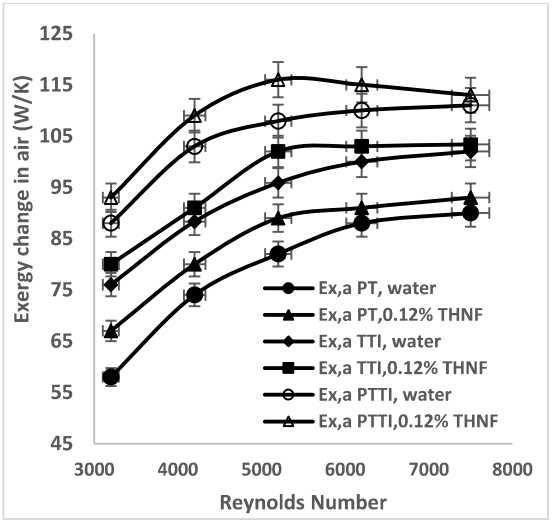

Fig. 5.21. Exergy change in air with Reynolds number for different inserts and working fluids.

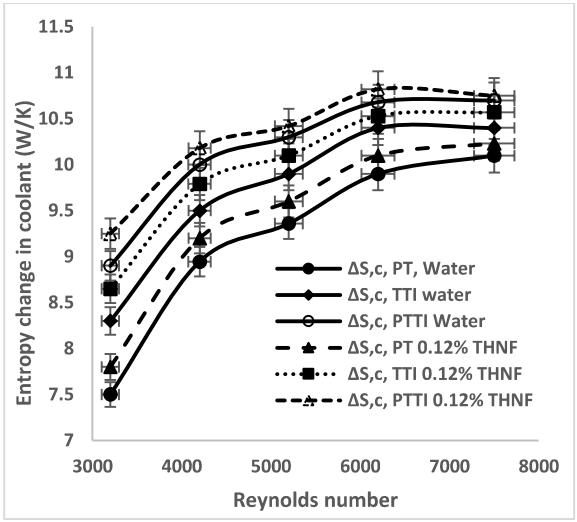

Fig. 5.22. Entropy change in coolant with Reynolds number for different inserts and working fluids.

Exergy variation for air with Reynolds number and for different fluids is presented in fig. 5.21. Exergy indicates the available energy and with an increment in Reynolds number exergy of air also increases. For geometrical inserts, exergy change in the air is higher for the PTTI case with 0.12% THNF working fluid and lowest obtained in the plain tube without inserts with water as working fluid due to the same reason stated in the explanation of increment of exergy change of coolant. The degradation of energy can be understood with entropy. Entropy analysis provides the greatest framework for understanding how to research energy consumption. Less energy is used

efficiently inside an HX the higher the entropy. Thermodynamically stated, HX with lower entropy should generally be favored. Entropy is a result of temperature change, pressure drop across the flow, and the heat exchange process for a fluid. The thermal change is extremely noticeable in low Reynolds numbers, but as the mass flow rate increases, the thermal change becomes less significant and viscous entropy takes over. Greater temperature change and pressure drop than other inserts tested are made possible by the presence of PTTI turbulators inserts, secondary flow, and vorticity. From Fig. 5.22., on the comparison, with 0.12% THNF, at 3200 Reynolds number, PTTI shows 23%, TTI shows 15% higher entropy compared to a plain tube with water as working fluid.

5.6.4 Effect of flow and inserts on Sustainability, Carbon discharge and HXOC

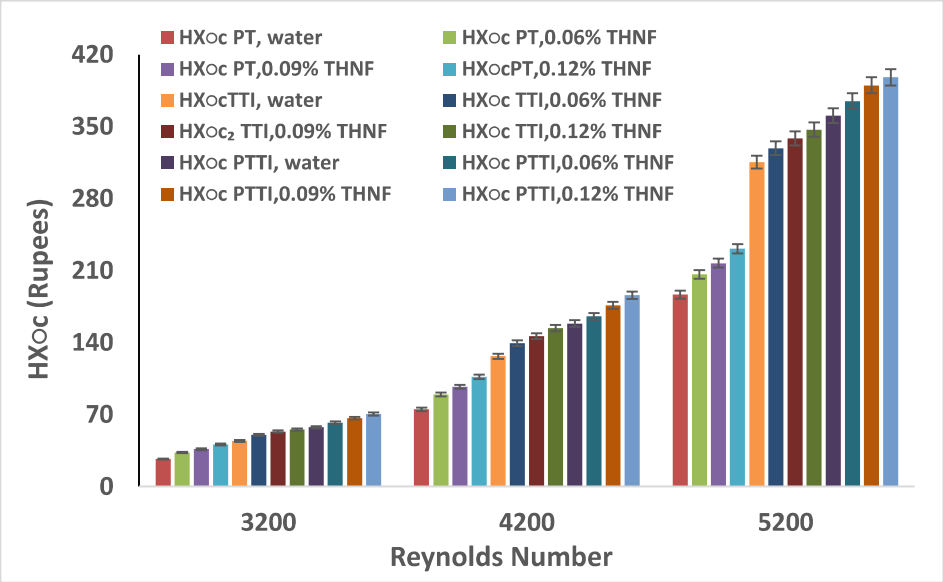

Fig. 5.23. Heat exchanger operating cost with Reynolds number for different inserts and working fluids.

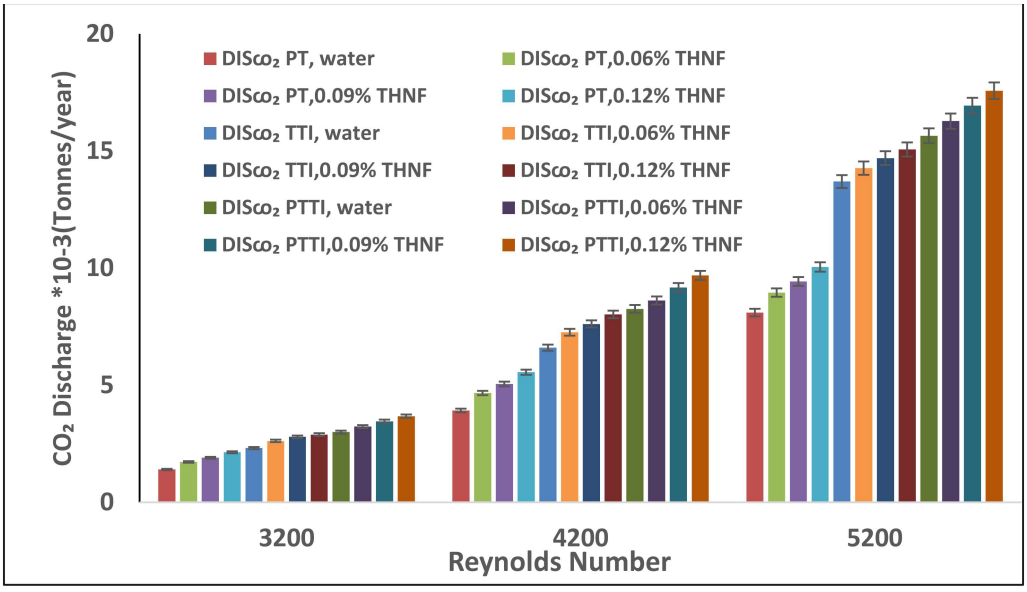

Fig. 5.24. Discharge of Carbon with Reynolds number for different inserts and working fluids.

The HX operating cost for various operating fluids of several geometrical inserts in a compact HX for three different Reynolds number is illustrated in Fig. 5.23. The assumption being the HX operates for 180 days in year before maintenance is carried. Heat exchanger operating cost is higher at a high Reynolds number due to higher pumping power and the relevant higher cost for the electricity consumption. Result reveals that with 0.12% THNF working fluid, PTTI requires 2.6 times, and TTI requires 2.1 times higher operating cost to run the pump continuously compared to the without inserts with water as working fluid. Also, the power supply required for the pump and fan to function, the electricity requirement may be fulfilled by an equivalent amount of coal to be burnt in terms of an annual CO_2 discharge. The annual CO_2 discharge to the environment for different working fluids and the three lower Reynolds number is shown in Fig. 5.24. The highest CO_2 discharge need of 10.4kg for DTTI HX is caused by HX operating for 180 days, whereas a minimum CO_2 discharge requirement of 5.2kg has been achieved without inserting HX. Additionally, related HX operating costs were looked into, which revealed a similar pattern of change in CO_2 discharge as it varied with THNFs and different inserts. The strength of the vorticity

is stronger in DTTI than PTTI even though it is missing in twisted tape inserts because the existence of the dimple form adds to the vorticity.

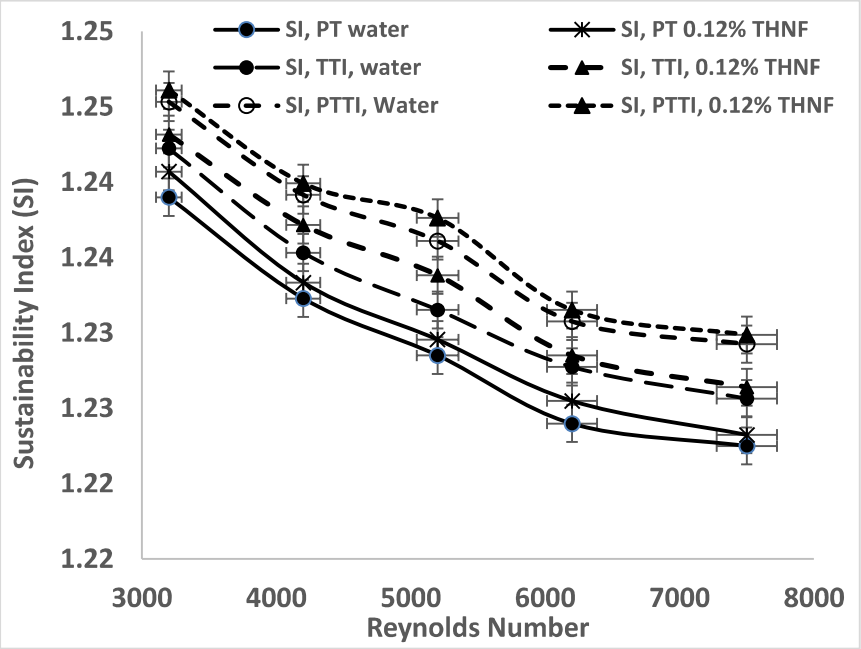

Fig. 5.25. Sustainability Index with Reynolds number for different inserts and working fluids.

Using coolant energy change and energy loss, a non-dimensional measure called SI can be used to calculate how effectively energy is being used. However, a study shows that SI rose as the coolant mass flow rate increased. Fig. 5.25. displays variation in SI for several HX turbulator inserts using numerous researched working fluids. When opposed to inserts, HX without inserts exhibits relatively reduced SI. As coolant (hot fluid) energy change, meanwhile, is greatest in the case of PTTI and lowest for without inserts, and modest for TTI. Due to a steeper thermal gradient normal to the fluid flow than TTI, PTTI produces a higher thermal change than TTI, and TTI lacks this additional flow restriction near the perforation positions. Thus, among the many turbulators examined, PTTI produced a true higher SI for all working fluid instances over a range of Reynolds number.

5.6.5 Effect of hybrid nanofluid on the performance parameters for selection of hybrid nanofluid

Different hybrid nanofluid is prepared and the measured thermophysical properties of hybrid nanofluid are listed in the Table 3.2. The performance parameter of the hybrid nanofluid is compared to the THNF at same volume concentration at fixed Reynolds number 3200, it is obtained that for same concentration, THNF shows higher heat transfer, second law efficiency,

Table. 5.4 Performance parameters for different hybrid nanofluid and THNF.

Parameters	**Water**	**CuO +TiO_2 /Water (0.12% v/v)**	**Al_2O_3+TiO_2/ Water (0.12% v/v)**	**Al_2O_3+TiO_2+CuO/ Water (0.12% v/v)**
Heat transfer (W)	3002	3205	3150	3290
Entropy generation rate(W/K)	1.20	1.25	1.23	1.27
Irreversibility (W)	366.6	379	370.5	384
Second law efficiency (%)	18.80	18.95	18.85	19.01
Performance Index	172	181	178	184
Exergy change of coolant (W)	402	439	425	450
Pressure drop (N/m^2)	68	79	75	81

performance index. Although the pressure drop and entropy also remain higher for the case of THNF, the coolant exergy is higher than the two different hybrid nanofluids investigated, also listed in the Table 5.4. Therefore, for the practical application and analysis, THNF at different concentrations has been explored more in the present investigation.

1.7 Highlights of the study

The present investigation focuses on the performance evaluation of the HX. Different working fluids are used as coolant in the tube. Geometrical modification and various turbulator inserts (Twisted inserts, perforated twisted inserts) are introduced in HX. The influence of geometrical inserts and different hybrid nanofluids with Reynolds number on performance parameters is also investigated. The key points of the present investigation are as follows:

- Under same coolant 0.12% (v/v) THNF, PTTI, and TTI achieve a maximum 28% and 19% higher heat transfer than without inserts in the heat exchanger at the lowest Reynolds number, respectively.
- TTI and PTTI show 50% and 88% higher friction factor than without inserts using water as a coolant, respectively.
- At the lowest Reynolds number 3200, TTI and PTTI increase 24% and 17% higher overall heat transfer coefficient with water as a coolant, respectively.
- PEC is highest at the lowest Reynolds number with PTTI and 0.12% (v/v) THNF as cooling agent 1.075, then followed by TTI 1.06.
- TTI and PTTI insert with 0.12% (v/v) THNF, shows 1.9% and 2.8% higher exergy efficiency compared to without inserts with water as a coolant, respectively.
- TTI in HX with 0.12% (v/v) THNF, requires 2.07 to 1.8 times higher operating cost while PTTI shows 2.63 to 2.13 times higher operating cost than without inserts with water as coolant.
- TTI and PTTI in HX (heat exchanger) with water as coolant releases 1.65 to 1.7 times and 2.14 to 1.9 times higher carbon discharge to the environment than without inserts.

- PTTI is more suitable to be used for better heat transfer improvement as passive device inserts.

This page is left intentionally blank